
New Trends in Electrical Engineering Automatic Control, Computing and Communication Sciences

Edited by

Carlos A. Coello Coello

Alexander Poznyak

José Antonio Moreno Cadenas

Vadim Azhmyakov

LOGOS Verlag, Berlin, Germany

Contents

Part I Automatic Control and Mechatronics

1 Error estimates of mixed finite element methods for semilinear optimal control problems <i>Zuliang Lu</i>	3
2 Sliding Mode Control Approach combined with Block Control for a Unified Power Flow Controller (UPFC) in a Small Power System <i>Fidel Robles-Aguirre, Alexander Loukianov, Leonid Fridman, J.M. Cañedo</i> ...	21
3 Closed-Loop Identification for a Velocity Controlled DC Servomechanism: Theory and Experiments <i>Rubtn Garrido, Roger Miranda</i>	41
4 Practical stability of neutral and retarded type time delay systems: LMI's approach <i>R. Villafuerte and S. Mondié</i>	53
5 Relationship Between Dynamic Programming and the Maximum Principle for Impulsive Hybrid LQ Optimal Control Problems <i>R Galvan-Guerra, V. Azhmyakov</i>	75
6 Task Space Robot Control Using Joint Proportional Action <i>Rubén Garrido, E. Alberto Canul, Alberto Soria</i>	93
7 Further Properties of Carleman Linearization <i>Irving Sánchez, Joaquín Collado</i>	107
8 Finite Element Modelling and Unbalance Compensation for an Asymmetrical Rotor-Bearing System with Two Disks <i>M. Arias-Montiel, G. Silva-Navarro</i>	127

9 Semiactive Control for the Unbalance Compensation in a Rotor-Bearing System <i>A. Cabrera-Amado, G. Silva-Navarro</i>	143
10 Design of a Passive/Active Autoparametric Pendulum Absorber for Damped Duffing Systems <i>G. Silva-Navarro, L. Macias-Czindapi, B. Vazquez-Gonzalez</i>	159

Part II Solid-State Materials and Electron Devices

11 Characterization of Nanocrystalline ZnO Grown on Silicon Substrates by DC Reactive Magnetron Sputtering <i>G. Juhrez-Diaz, A. Esparza-Garcia, M. Briseño-García, G. Romero-Paredes R., J. Martinez-Juhrez, R. Peña-Sierra</i>	179
12 Thermodynamic Stability of $A^{\text{III}}B_x^{\text{V}}C_y^{\text{V}}D_{1-x-y}^{\text{V}}$ Semiconductor Alloys <i>Salvador F. D. Albarrán, Alicia G. G. Noguez, Patricia R Peralta, Vyacheslav A. Elyukhin</i>	193
13 Electrical, Relaxation and Crystallization Properties of Ge₂Sb₂Te₅ Alloys <i>E. Morales-Shnchez, E. Prokhorov, G. Trapaga, M. A. Hernández-Landaverde, J. González-Hernández</i>	207

Part III Biomedical Engineering, Circuits and Communication Systems

14 Suitability of Alternative Methods of Time Delay Measurements for Ultrasonic Noninvasive Temperature Estimation in Oncology Hyperthermia <i>Arturo Vera, Lorenzo Leija, Abraham Tellez, Ivonne Bazhn, Antonio Ramos</i> ...	223
15 Assessing the Statistical Nature of the MAI in a WSN based on IR-UWB for Cognitive-like Operation <i>Fernando Ramirez-Mireles, Angel Almada</i>	249
16 Hybrid Space-Time Codes for MIMO Wireless Communications <i>Joaquin Cortez, Alberto Sanchez, Miguel Bazdresch, Omar Longoria, Ramon Parra</i>	267
17 Calculation of the Radiation Pattern of On-Board Antennas Placed over Complex Structures using Physical Optics Including the Contribution of the Shadowed Areas <i>Lorena Lozano, Francisco Saez de Adana, Manuel Felipe Cátedra</i>	289

Thermodynamic Stability of $A^{III}B_x^VC_y^VD_{1-x-y}^V$ Semiconductor Alloys

Salvador F. D. Albarrán¹, Alicia G. G. Noguez², Patricia R. Peralta¹, and Vyacheslav A. Elyukhin³

¹ Department of Engineering in Computation, ESIME-IPN Culhuacan, Av. Santa Ana 1000, Mtxico D. F., 04430

² Department of Radioactive Facilities CNSNS, Dr. José Ma. Barragán 779, Mtxico D. F., 03020

³ Department of Electrical Engineering, CINVESTAV-IPN, Av. IPN 2508, México D. F., 07360
e-mail: felipondiaz@hotmail.com

Summary. Spinodal decomposition of the $GaSb_xN_yAs_{1-x-y}$ quaternary alloys lattice-matched to the GaAs as the result of the internal deformation and coherency strain energies is described. The alloys are represented as quaternary regular solutions. The internal deformation energy is represented by interaction parameters between the constituent compounds estimated within the framework of the valence force field model. Ranges of spinodal decomposition of the $GaSb_xN_yAs_{1-x-y}$ alloys up to $y \leq 0.035$ with and without coherency strain energy are demonstrated.

12.1 Introduction

Dilute nitride III-V alloys have attracted a lot of attention since the last decade. The earliest studies were initiated a long time ago on N-doped GaP, with nitrogen concentration in the range $10^{17} - 10^{18} \text{ cm}^{-3}$ [1]. In this material, narrow photoluminescence lines were attributed to excitons bounded to isolated N centres or N-N pairs [1]. In the early 1990s, the development of wide-gap nitrides has considerably influenced the technology of N sources and precursors. As a consequence, new investigations on N-containing III-V were carried out from 1992, with modern epitaxial growth techniques. N concentrations around 1% and above could be easily achieved in GaAs or GaP. The introduction of nitrogen in GaAs also results in a smaller lattice parameter. Therefore, a dilute amount of nitrogen offers a unique feature of reducing simultaneously the band gap and the lattice parameter of a given III-V alloy [1].

It has been found that incorporating low concentrations of N has a profound effect on the electronic properties of the III-V alloy semiconductors composed of (B, Al, Ga, In) (N, P, As, Sb) [2]. A reduction on the band gap exceeding 0.1 eV per atomic percent of N content was observed in GaN_xAs_{1-x} for $x < 0.015$ [3]. Model calculations of the band structure of some of the group III-N-V alloys have shown

that the reduction of the band gap is due to the highly localized nature of the perturbation introduced by N atoms [4]. The $\text{GaSb}_x\text{N}_y\text{As}_{1-x-y}$ material system was recently proposed as promising candidate for GaAs-based optoelectronic devices. Compared to InGaAs , the $\text{GaSb}_x\text{N}_y\text{As}_{1-x-y}$ material system has the advantage that for the same wavelength, GaAsSb has lower compressive strain compared to InGaAs .

The large difference between the atomic sizes of nitrogen, antimony and arsenic gives rise to the significant strain energy of such alloys. The internal deformation energy provides the tendency to disintegration that can lead to the appearance of the thermodynamically unstable states with respect to the phase separation [5]. The thermodynamically unstable states with respect to the decomposition may be realized as spinodal decomposition [5]. Spinodal decomposition results in formation of the macroscopic phases of different compositions decreasing the internal energy of the alloy [5]. At the same time, this decomposition leads to an occurrence of the coherency strain energy due to the stress between both formed regions with different compositions and these regions and other part of alloy [6]. Thus, the internal deformation and coherency strain energies are two origins controlling spinodal decomposition in the $\text{GaSb}_x\text{N}_y\text{As}_{1-x-y}$ semiconductor alloys. The aim of our chapter is the consideration of the spinodal decomposition region of $\text{GaSb}_x\text{N}_y\text{As}_{1-x-y}$ layers grown on $\text{GaAs}(001)$ substrates with all the described above origins. In the next section we briefly describe these solutions or alloys.

12.2 $\text{GaSb}_x\text{N}_y\text{As}_{1-x-y}$ Quaternary Alloys

$\text{GaSb}_x\text{N}_y\text{As}_{1-x-y}$ belong to $\text{AB}_x\text{C}_y\text{D}_{1-x-y}$ - type alloys where the anions (Sb, N and As) are surrounded by only one type cation (Ga), having one mixed sublattice. When we consider the chemical composition of such alloys the sum of the concentrations of the atoms in the mixed sublattice is supposed equal to unit. In the notation $\text{GaSb}_x\text{N}_y\text{As}_{1-x-y}$, x is the concentration of Sb atoms and y is the concentration of N atoms. As a result, $\text{GaSb}_x\text{N}_y\text{As}_{1-x-y}$ alloys have three types chemical bonds: Ga-Sb, Ga-N and Ga-As. Therefore, they are known as quaternary alloys of three binary compounds or quasiternary alloys since these alloys consist of three types of the chemical substances.

A special feature of these alloys is the one to one correspondence between the concentrations of the atoms and chemical bonds. This one to one correspondence can be written as

$$x_{\text{GaSb}} = x, \quad (12.1)$$

$$x_{\text{GaN}} = y, \quad (12.2)$$

$$x_{\text{GaAs}} = 1 - x - y. \quad (12.3)$$

We can also represent the crystal structure of these quaternary alloys as a structure consisting of molecules of the binary compounds. Concentrations of the bonds in the quaternary solutions of three binary compounds are also independent on the arrangement of the atoms in the mixed sublattice. In other words, the correlations in the

arrangement of the atoms in the mixed sublattice do not affect the concentrations of the chemical bonds or the chemical composition of such solutions. These characteristics offer an advantage over other quaternary alloys represented as $A_xB_{1-x}C_yD_{1-y}$. Their crystal lattice consists of the mixed cation and anion sublattices, since two kinds of the atoms fill each of them. As a result, $A_xB_{1-x}C_yD_{1-y}$ alloys have four types of chemical bonds: A-C, A-D, B-C and B-D.

A special peculiarity of these alloys is the transformation of the A-C and B-D bonds in the A-D and B-C bonds or vice versa. This property is independent of the concentrations x and y . Therefore, the spinodal decomposition is accompanied by the transformation of the bonds and it modifies the chemical composition and should change the free energy of the alloy [7]. For example, spinodal decomposition range of the $In_xGa_{1-x}N_yAs_{1-y}$ alloys depends on the strain and coherency strain energies and transformation of the bonds. As it was shown in [8], the very extensive spinodal decomposition range of the $In_xGa_{1-x}N_yAs_{1-y}$ lattice mismatched to GaAs occurs due to the exchange of atoms. Then, there is one mixed sublattice in the crystal structure of the $GaSb_xN_yAs_{1-x-y}$ alloys in comparison to the $In_xGa_{1-x}N_yAs_{1-y}$ alloys. Mixing in one sublattice only should lead to the smaller internal deformation energy. We can say that from the spinodal decomposition standpoint, the $GaSb_xN_yAs_{1-x-y}$ alloys should be a more perspective material than the $In_xGa_{1-x}N_yAs_{1-y}$ alloys.

As mentioned above the internal deformation and coherency strain energies are two mechanisms controlling the decomposition in the $GaSb_xN_yAs_{1-x-y}$ quaternary alloys. The internal deformation energy is described by the valence force field approach. This approach is very important in our study on the spinodal decomposition, so we explain this model.

12.3 Valence Force Field Approach

The most useful phenomenological description of the short-range valence forces in the tetrahedrally coordinated crystals is the valence-force-field (VFF) approach, in which all interatomic forces are resolved into bond-stretching and bond-bending forces [9]. The are two primary virtues of the VFF model. First, because all distortions are described in terms of bond lengths and angles, the model is automatically rotationally invariant so that serious errors that may arise in the ordinary force-constant approach are avoided [10]. Second, in crystals in which atom pair bonds play an essential role, the VFF model is the most natural description of interatomic forces. Thus one expects the VFF model to involve the smallest possible number of parameters. In other words, the VFF model described the strained state of the elemental semiconductors or binary compounds by using two microscopic elastic constant. The deformation energy of the primitive or unit cell of the binary compounds with the zinc blende structure according to the VFF model is given as

$$u = \frac{1}{2} \alpha \left(\frac{3}{4R^2} \right) \sum_{i=1}^4 [\Delta (r_i^1 \cdot r_i^1)]^2 + \frac{1}{2} \sum_{s=1}^2 \beta^s \left(\frac{3}{4R^2} \right) \sum_{i,j>i} [\Delta (r_i^s \cdot r_j^s)]^2 \quad (12.4)$$

where α and β are the bond-stretching and bond-bending elastic constants, R is the bond length in undistorted crystal, $\mathbf{A}(\mathbf{r}_i^1 \cdot \mathbf{r}_i^1) = R_i^2 - r_i^2$ and $\mathbf{A}(\mathbf{r}_i^s \cdot \mathbf{r}_j^s) = R^2 \cos \varphi_0 - \mathbf{r}_i^s \mathbf{r}_j^s \cos \varphi$ are the scalar variations, \mathbf{r}_{ij}^s are bond vectors about atom s , $\varphi_0 = 109.47^\circ$ and φ are the angles between the bonds in the unstrained and strained crystal, respectively [9].

The expressions for the elastic constants have the simple form [9]

$$C_{11} + 2C_{12} = \frac{\sqrt{3}}{4R}(3\alpha + \beta) - 0.355SC_0, \quad (12.5)$$

$$C_{11} - C_{12} = \frac{\sqrt{3}}{R}\beta + 0.53SC_0, \quad (12.6)$$

$$C_{44} = \frac{\sqrt{3}}{4R}(\alpha + \beta) - 0.136SC_0 - C\zeta^2, \quad (12.7)$$

where

$$C = \frac{\sqrt{3}}{4R}(\alpha + \beta) - 0.266SC_0, \quad (12.8)$$

and

$$\zeta = C^{-1} \left[\frac{\sqrt{3}}{4R}(\alpha - \beta) - 0.294SC_0 \right]. \quad (12.9)$$

In particular (5), (6) and (9) may be used to derive a expression for the internal strain parameter

$$\zeta = \frac{2C_{12} - \mathcal{C}}{C_{11} + C_{12} - \mathcal{C}}, \quad (12.10)$$

where

$$\mathcal{C} = 0.314SC_0. \quad (12.11)$$

Thus, the equations (5)-(9) predict a relation among the elastic constants which may be checked experimentally. The relation may be written

$$\frac{2C_{44}(C_{11} + C_{12} - \mathcal{C})}{(C_{11} - C_{12})(C_{11} + 3C_{12} - 2\mathcal{C}) + 0.831\mathcal{C}(C_{11} + C_{12} - \mathcal{C})} = 1. \quad (12.12)$$

Now the internal deformation energy is represented by the interaction parameters between the constituent compounds of the $\text{GaSb}_x\text{N}_{1-x}\text{As}_{1-x-y}$ alloys. The interaction parameters were obtained from the strain energies of the corresponding ternary alloys estimated by (4).

12.3.1 Strain Energy of the $\text{A}_x\text{B}_{1-x}\text{C}$ Ternary Alloys

The basic unit of the crystal lattice of the $\text{A}_x\text{B}_{1-x}\text{C}$ ternary alloys in our description is a tetrahedral cell with four atoms at the vertices and one atom inside. The atoms at the vertices are the atoms of the mixed sublattice and one atom inside such cell is an atom from another sublattice. There are five types of tetrahedral cells: $4\text{A}1\text{C}$, $3\text{A}1\text{B}1\text{C}$,

2A2B1C, 1A3B1C and 4B1C. It is supposed that the cells of any types have the same distances between the vertices because the mixed sublattice is slightly distorted. It is very important point for further description. Figure 1 shows the tetrahedral cells.

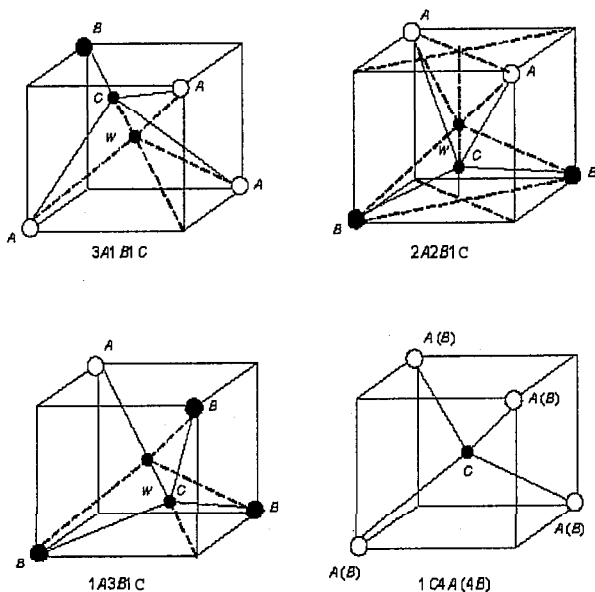


Fig. 12.1. 4A4(B)1C, 3A1B1C, 2A2B1C, 1A3B1C tetrahedral cells

The displacements of the central atom C are calculated by the minimum condition of the deformation energy of the cells. Average distances between the nearest atoms in the $A_xB_{1-x}C$ ternary alloy are written as

$$\overline{R_{AC}} = x^3 R_{AC}^{4A1C} + 3x^2(1-x) R_{AC}^{3A1B1C} + 3x(1-x)^2 R_{AC}^{2A2B1C} + (1-x)^4 R_{AC}^{1A3B1C}, \quad (12.13)$$

$$\overline{R_{BC}} = x^3 R_{BC}^{3A1B1C} + 3x^2(1-x) R_{BC}^{2A2B1C} + 3x(1-x)^2 R_{BC}^{1A3B1C} + (1-x)^4 R_{BC}^{4B1C}. \quad (12.14)$$

Where R_{AC}^{4A1C} is the distance between the A and C atoms in the 4A1C tetrahedral cell. The random distribution of the atoms in the mixed sublattice was taken account to obtain these formulas. The strain energies of the tetrahedral cells of the $A_xB_{1-x}C$ alloys are

$$u_{4A1C} = 2(1-x)^2 r^2 (3\alpha_{AC} + \beta_{AC}), \quad (12.15)$$

$$u_{3A1B1C} = \frac{3}{2} \left\{ 3\alpha_{AC} \left[(1-x)r - \frac{w_{3A1B}}{3} \right]^2 + \alpha_{BC} (xr - w_{3A1B})^2 \right\} + \frac{\beta_{AC} + \beta_{BC}}{8} [(1-2x)r - 2w_{3A1B}]^2 + \beta_{AC} [(1-x)r - w_{3A1B}]^2, \quad (12.16)$$

$$u_{2A2B1C} = 3 \left\{ \alpha_{AC} \left[(1-x)r - \frac{w_{2A2B}}{\sqrt{3}} \right]^2 + \alpha_{BC} \left(xr - \frac{w_{2A2B}}{\sqrt{3}} \right)^2 \right\} + \frac{\beta_{AC}}{3} [(1-x)r + \sqrt{3}w_{2A2B}]^2 + \frac{\beta_{AC}}{3} (xr + \sqrt{3}w_{2A2B})^2 + \frac{\beta_{AC} + \beta_{BC}}{6} (1-2x)r^2, \quad (12.17)$$

$$u_{1A3B1C} = \frac{3}{2} \left\{ \alpha_{AC} [(1-x)r - w_{1A3B}]^2 + 3\alpha_{BC} \left(xr - \frac{w_{1A3B}}{3} \right)^2 \right\} + \frac{3}{2} \left\{ \frac{\beta_{AC} + \beta_{BC}}{8} [(1-2x)r + 2w_{1A3B}]^2 + \beta_{BC} (xr + w_{1A3B})^2 \right\}, \quad (12.18)$$

$$u_{4B1C} = 2x^2 r^2 (3\alpha_{BC} + \beta_{BC}), \quad (12.19)$$

$$u_{4A1C} = 0. \quad (12.20)$$

and the displacements of the central C atoms

$$w_{3A1B1C} = \frac{3[\alpha_{AC} + (\alpha_{BC} - \alpha_{AC})x] + \frac{5\beta_{AC} + \beta_{BC}}{2} - (3\beta_{AC} + \beta_{BC})x}{\alpha_{AC} + 3\alpha_{BC} + 3\beta_{AC} + \beta_{BC}} r, \quad (12.21)$$

$$w_{2A2B1C} = \sqrt{3} \frac{\alpha_{AC}(1-x) + \alpha_{BC}x - \frac{\beta_{AC}}{3}(1-x) - \frac{\beta_{BC}}{3}x}{\alpha_{AC} + \alpha_{BC} + \beta_{AC} + \beta_{BC}} r, \quad (12.22)$$

$$w_{1A3B1C} = \frac{3[\alpha_{AC} + (\alpha_{BC} - \alpha_{AC})x] - \frac{\beta_{AC} + \beta_{BC}}{2} + (\beta_{AC} - \beta_{BC})x}{3\alpha_{AC} + 3\alpha_{BC} + \beta_{AC} + 3\beta_{BC}} r, \quad (12.23)$$

$$u_{4B1C} = 0. \quad (12.24)$$

Where $r = R_{AC} - R_{BC}$, R_{AC} is the distance between A and C atoms in the \bar{AC} unstrained compound, α_{AC} and β_{AC} are the bond length and bond-angle elastic constants of AC compound, respectively, w_{3A1B1C} is the displacement of central atom C in the 3A1B1C tetrahedral cell from the geometrical center of this cell. The supposition that the bond-angle elastic constant between the AC and BC bonds is equal arithmetical average of the bond-angle elastic constants of the AC and BC compounds

$$\beta_{AC-BC} = \frac{\beta_{AC-AC} + \beta_{BC-BC}}{2}, \quad (12.25)$$

is used in the formulas of the displacements of the central atoms and deformation energies.

After calculation the deformation energies of all types of the tetrahedral cells we can calculate the average deformation energy of a tetrahedral cell which is given as

$$\bar{u} = x^4 u_{4A1C} + 4x^3(1-x)u_{3A1B1C} + 6x^2(1-x)^2 u_{2A2B1C} + (1-x)^3 u_{1A3B1C} + (1-x)^4 u_{4B1C}. \quad (12.26)$$

12.4 Coherency Strain Energy

Hooke's Law states that

$$\epsilon = s\sigma, \quad (12.27)$$

where s is a constant. s is called the elastic compliance constant or, shortly, the compliance. As an alternative we could write

$$\sigma = C\epsilon, \quad (12.28)$$

with

$$C = \frac{1}{s}, \quad (12.29)$$

where C is the elastic stiffness constant, or the stiffness. C is also Young's Modulus [11]. The generalized form of Hooke's Law may be written as

$$\epsilon_{ij} = s_{ijkl}\sigma_{kl}, \quad (12.30)$$

the s_{ijkl} are the compliances of the crystal. Equation (30) stands for nine equations, for example, $\epsilon_{11} = s_{1111}\sigma_{11} + s_{1112}\sigma_{12} + s_{1113}\sigma_{13} + s_{1121}\sigma_{21} + s_{1122}\sigma_{22} + s_{1123}\sigma_{23} + s_{1131}\sigma_{31} + s_{1132}\sigma_{32} + s_{1133}\sigma_{33}$ and each with nine terms on the right-hand side. There are 81 s_{ijkl} coefficients.

As an alternative to (30) the stresses may be expressed in terms of the strains [11] by the equations

$$\sigma_{ij} = C_{ijkl}\epsilon_{kl}, \quad (12.31)$$

where the C_{ijkl} are the 81 stiffness constants of the crystal. However, C_{ijkl} is a fourth-rank tensor that satisfies the equalities

$$C_{ijkl} = C_{jikl}, \quad (12.32)$$

and

$$C_{ijkl} = C_{jilk}. \quad (12.33)$$

The equations (32) and (33) reduce the number of independent C_{ijkl} from 81 to 36. Therefore, (30) takes the shorter form

$$\sigma_i = C_{ij}\epsilon_j \quad (i, j = 1, 2, \dots, 6), \quad (12.34)$$

it may be written in matrix notation as

$$\begin{pmatrix} \sigma_1 \\ \vdots \\ \sigma_6 \end{pmatrix} = \begin{pmatrix} C_{11} & C_{12} & \cdots & C_{16} \\ \vdots & \vdots & \ddots & \vdots \\ C_{61} & C_{62} & \cdots & C_{66} \end{pmatrix} \begin{pmatrix} \epsilon_1 \\ \vdots \\ \epsilon_6 \end{pmatrix}. \quad (12.35)$$

An important application of (35) is for cubic crystals [12]. In this case we have

$$\begin{pmatrix} \sigma_x \\ \sigma_y \\ \sigma_z \\ \tau_{xy} \\ \tau_{yz} \\ \tau_{zx} \end{pmatrix} = \begin{pmatrix} C_{11} & C_{12} & C_{12} & 0 & 0 & 0 \\ C_{12} & C_{11} & C_{12} & 0 & 0 & 0 \\ C_{12} & C_{12} & C_{11} & 0 & 0 & 0 \\ 0 & 0 & 0 & C_{44} & 0 & 0 \\ 0 & 0 & 0 & 0 & C_{44} & 0 \\ 0 & 0 & 0 & 0 & 0 & C_{44} \end{pmatrix} \begin{pmatrix} \varepsilon_x \\ \varepsilon_y \\ \varepsilon_z \\ \gamma_{xy} \\ \gamma_{yz} \\ \gamma_{zx} \end{pmatrix}, \quad (12.36)$$

where the ε_i s and σ_i s are the normal strain and stresses, respectively, and the γ_{ij} s and τ_{ij} s are the shear strains and stresses, respectively.

If the epitaxial **film** and its substrate are oriented along one of the (100) cubic symmetry directions, then (36) reduces to

$$\begin{pmatrix} \sigma_{\parallel} \\ \sigma_{\perp} \end{pmatrix} = \begin{pmatrix} C_{11} + C_{12} & C_{12} \\ 2C_{12} & C_{11} \end{pmatrix} \begin{pmatrix} \varepsilon_{\parallel} \\ \varepsilon_{\perp} \end{pmatrix}, \quad (12.37)$$

by [12], if the epitaxial film has a free surface, then

$$\sigma_{\perp} = 0, \quad (12.38)$$

and the perpendicular strain of the **film** is

$$\varepsilon_{\perp} = \frac{-2C_{12}}{C_{11}} \varepsilon_{\parallel}, \quad (12.39)$$

whereas the parallel componente is given as

$$\sigma_{\parallel} = \frac{(C_{11} - C_{12})(C_{11} + 2C_{12})}{C_{11}} \varepsilon_{\parallel}. \quad (12.40)$$

Therefore, the coherency strain energy of the $AB_xC_yD_{1-x-y}$ quaternary alloys may be written as the elastic energy of two epitaxial layers lattice-mismatched with the substrate that is given as [12]

$$u^L = \sum_{i=1}^2 \gamma_i v_i \frac{(C_{11}^i - C_{12}^i)(C_{11}^i + 2C_{12}^i)}{C_{11}^i} \left(\frac{a_i - a_{\text{sub}}}{a_{\text{sub}}} \right)^2. \quad (12.41)$$

Where γ_i , v_i and a_i are the portion, molar volume and the lattice-parameter of the i th phase of the alloy estimated by the Vegards Law, C_{11}^i and C_{12}^i , are expressed as

$$C_{11}^i = xC_{11}^{AB} + yC_{11}^{AC} + (1-x-y)C_{11}^{AD}, \quad (12.42)$$

$$C_{12}^i = xC_{12}^{AB} + yC_{12}^{AC} + (1-x-y)C_{12}^{AD}. \quad (12.43)$$

The minimum value of the coherency energy u^L is achieved at the condition $\gamma_1 = \gamma_2$.

12.5 Spinodal Decomposition in the $\text{GaSb}_x\text{N}_y\text{As}_{1-x-y}$ Alloys

According to Gibbs classic treatment of phase stability, spinodal decomposition begins from the changes that are large in extent but small in degree [13] and develops when a negligibly small phase separation fluctuation decreases the free energy of an alloy. The initial stage of spinodal decomposition is accompanied by transfer of atoms on the distances of order of a lattice parameter. It was shown [14] that in cubic crystals the spinodal decomposition forms of the layers in a plane where their elastic energy is minimal. Accordingly, the transfer of atoms lead to an occurrence of thin two-layer region with negligibly small distinction in the composition. The composition of the formed layers at the initial stage of the decomposition can be considered as constant values due to their small thickness.

As the decomposition is developed the transfer of atoms and thickness of the layers become larger and composition of the layers varies with tickness. Afterwards, the difference in the mean concentrations of the phases is increased continuously [15]. The $\text{GaSb}_x\text{N}_y\text{As}_{1-x-y}$ quaternary alloys contain three types of the chemical bonds and the amounts of them are kept at the disintegration. Therefore, the Helmholtz free energy of mixing of the alloy is only varied at spinodal decomposition. In the cubic crystals minimal elastic energy corresponds the (100) planes if relation

$$2C_{44} - C_{11} + C_{12} > 0 . \quad (12.44)$$

Between the stiffness coefficients is fulfilled [5]. Thus, the initial stage of spinodal decomposition in the $\text{GaSb}_x\text{N}_y\text{As}_{1-x-y}$ alloys is considered as appearance thin two-layer objects oriented in the (100) plane.

The disintegration changes the value x, y or both of them in emerging two phases of the decomposed alloy. The variation of the Helmholtz free energy of mixing at the initial stage of spinodal decomposition can be represented as

$$\begin{aligned} \delta f \approx & \frac{1}{2} \frac{\partial^2}{\partial x^2} [f^M(x, y) + u^L(x, y)] (\delta x)^2 + \\ & \frac{\partial^2}{\partial x \partial y} [f^M(x, y) + u^L(x, y)] (\delta x)(\delta y) + \\ & \frac{1}{2} \frac{\partial^2}{\partial y^2} [f^M(x, y) + u^L(x, y)] (\delta y)^2 . \end{aligned} \quad (12.45)$$

An alloy reaches the spinodal decomposition range when the variation of its free energy becomes equal to zero [16]

$$\delta f = 0 . \quad (12.46)$$

This condition is fulfilled if one of two expressions

$$\frac{\partial^2 f}{\partial x^2} , \quad (12.47)$$

$$\frac{\partial^2 f}{\partial x^2} \times \frac{\partial^2 f}{\partial y^2} - \left(\frac{\partial^2 f}{\partial x \partial y} \right)^2. \quad (12.48)$$

Is equal to zero [17]. The Helmholtz free energy of the homogeneous alloys grown on crystalline substrates can be represented as a sum

$$f = f^C + u^S + u^L - Ts, \quad (12.49)$$

where f^C , u^S , u^L are the free energy of the constituent compounds strain and lattice mismatch energies, respectively, s is the configurational entropy, and T is the absolute temperature. The negligibly small lattice mismatch between the alloy and substrate is introduced in order to include the coherency strain energy in our consideration.

The free energy of the constituent compounds of $\text{GaSb}_x\text{N}_y\text{As}_{1-x-y}$ is given as

$$f^C = x\mu_{\text{GaSb}}^0 + y\mu_{\text{GaN}}^0 + (1-x-y)\mu_{\text{GaAs}}^0. \quad (12.50)$$

Where μ_{GaSb}^0 is the chemical potential of GaSb in the standard state. The internal deformation energy of the alloy is written as

$$u^C = xy\alpha_{\text{GaSb-GaN}} + x(1-x-y)\alpha_{\text{GaSb-GaAs}} + y(1-x-y)\alpha_{\text{GaN-GaAs}}. \quad (12.51)$$

Where $\alpha_{\text{GaSb-GaN}}$ is the interaction parameter between binary compounds GaSb and GaN. Thus, the internal deformation energy is represented by the interaction parameters between the constituent compounds of such alloys (section 2) [18].

The coherency strain energy of the decomposed alloy may be written as the elastic energy of two epitaxial layers lattice mismatched with the GaAs (001) substrate that is given by (41) with $a_{\text{sub}} = a_{\text{GaAs}}$. The configurational entropy of the alloy considered is obtained by the formula

$$s = k_B \ln g, \quad (12.52)$$

where g is the degeneracy factor. The expression for the factor g is

$$g = \frac{(N_{\text{Sb}} + N_{\text{N}} + N_{\text{As}})!}{N_{\text{Sb}}!N_{\text{N}}!N_{\text{As}}!}, \quad (12.53)$$

where N_{Sb} , N_{N} and N_{As} are the numbers of atoms Sb, N and As, respectively. Therefore, the configurational entropy of $\text{GaSb}_x\text{N}_y\text{As}_{1-x-y}$ can be expressed as

$$s = -R[x \ln x + y \ln y + (1-x-y) \ln(1-x-y)]. \quad (12.54)$$

Equations (46) and (47) after taking into account the formulas (41), (48-50) and (52) are given, respectively, by

$$-2\alpha_{\text{GaSb-GaAs}} + RT \frac{1-y}{x(1-x-y)} + \frac{\partial^2 u^L}{\partial x^2} = 0, \quad (12.55)$$

and

$$\begin{aligned}
& \left[-2\alpha_{\text{GaSb-GaAs}} + RT \frac{1-y}{x(1-x-y)} + \frac{\partial^2 u^L}{\partial x^2} \right] \times \\
& \left[-2\alpha_{\text{GaN-GaAs}} + RT \frac{1-x}{y(1-x-y)} + \frac{\partial^2 u^L}{\partial y^2} \right] - \quad (12.56) \\
& \left[\alpha_{\text{GaSb-GaN}} - \alpha_{\text{GaSb-GaAs}} - \alpha_{\text{GaN-GaAs}} + \frac{RT}{1-x-y} + \frac{\partial^2 u^L}{\partial x \partial y} \right]^2 = 0 .
\end{aligned}$$

Where R is the universal gaseous constant.

12.6 Results

The spinodal decomposition ranges for the $\text{GaSb}_x\text{N}_y\text{As}_{1-x-y}$ quaternary alloys lattice matched to GaAs with and without taking into account the coherency strain energy are demonstrated in the Fig. 2. As can be seen, the coherency strain energy emerging in the disintegration alloy substantially decreasing the temperature of spinodal decomposition. Therefore, the spinodal decomposition region of the alloy is narrower when we consider the coherency strain. $\text{GaSb}_{0.07}\text{N}_{0.023}\text{As}_{0.907}$ ($a = 5.655 \text{ \AA}$, $\lambda = 1300 \text{ nm}$) alloys [19] is outside the spinodal decomposition range at its growth temperature. In the figure, this experimental value is represented by a circle.